In vivo imaging characterization of basal cell carcinoma and cutaneous response to high-dose ionizing radiation therapy: A prospective study of reflectance confocal microscopy, dermoscopy, and ultrasonography

Cristian Navarrete-Dechent, MD,[a,b] Miguel Cordova, MD,[b] Konstantinos Liopyris, MD,[b] Saud Aleissa, MD,[b] Milind Rajadhyaksha, PhD,[b] Gil'ad Cohen, MS,[c] Ashfaq A. Marghoob, MD,[b] Anthony M. Rossi, MD,[b] and Christopher A. Barker, MD[d]

Santiago, Chile and New York, New York

Background: Radiation therapy (RT) is a treatment option for select skin cancers. The histologic effects of RT on normal skin or skin cancers are not well characterized. Dermoscopy, high-frequency ultrasonography (HFUS), and reflectance confocal microscopy (RCM) are noninvasive imaging modalities that may help characterize RT response.

Objectives: To describe changes in the tumor and surrounding skin of patients with basal cell carcinoma (BCC) treated with RT.

Methods: The study was conducted between 2014 and 2018. Patients with biopsy-proven BCCs were treated with 42 Gy in 6 fractions using a commercially available brachytherapy device. Dermoscopy, HFUS, and RCM were performed before treatment and at 6 weeks, 3 months, and 12 months after RT.

Results: A total of 137 imaging assessments (RCM + dermoscopy + HFUS) were performed in 12 patients. BCC-specific features were present in 81.8%, 91%, and 17% of patients imaged with dermoscopy, RCM, and HFUS at baseline, respectively, before treatment. After treatment, the resolution of these features was noted in 33.4%, 91.7%, and 100% of patients imaged with the respective modalities. No recurrences were seen after a mean of 31.7 months of follow-up.

Limitations: Small sample size and no histopathologic correlation.

From the Department of Dermatology, Escuela de Medicina, Pontificia Universidad Católica de Chile, Santiago[a]; Dermatology Service, Department of Medicine, Memorial Sloan-Kettering Cancer Center, New York[b]; Medical Physics, Memorial Sloan Kettering Cancer Center, New York[c]; and Brachytherapy Service, Department of Radiation Oncology, Memorial Sloan Kettering Cancer Center, New York.[d]

Funding sources: Supported in part by the National Institutes of Health/National Cancer Institute Cancer Center Support Grant P30 CA008748 and in part by Elekta. The funders played no role in any aspect of the study.

Disclosure: Dr Rossi has no relevant conflicts of interest related to this article but has received grant funding from The Skin Cancer Foundation and the A. Ward Ford Memorial Grant for research related to this work and has also served on the advisory board or as a consultant or has given educational presentations for Allergan, Galderma, Evolus, Elekta, Biofrontera, Quantia, Merz, Dynamed, Skinuvia, Perf-Action, and LAM Therapeutics. Dr Barker's institution receives financial support from Elekta for research related to this work; outside of this work, his institution also receives financial support for Amgen and Merck, and in the last year, he has received honoraria from Regeneron for participating in an advisory board meeting. Drs Navarrete-Dechent, Cordova, Liopyris, Aleissa, and Rajadhyaksha; Author Cohen; and Dr Marghoob have no conflicts of interest to declare.

IRB approval status: Review and approved by Memorial Sloan Kettering Cancer Center (protocol #14-001).

Accepted for publication July 3, 2020.

Reprints not available from the authors.

Correspondence to: Christopher A. Barker, MD, Department of Radiation Oncology, Memorial Sloan Kettering Cancer Center, 1250 First Ave, New York, NY 10065. E-mail: barkerc@mskcc.org.

Published online August 20, 2020.

0190-9622/$36.00

https://doi.org/10.1016/j.jaad.2020.07.130

Conclusion: Dermoscopy and HFUS were not as reliable as RCM at characterizing BCC RT response. (J Am Acad Dermatol 2021;84:1575-84.)

Key words: basal cell carcinoma; brachytherapy; dermatoscopy; dermoscopy; radiation therapy; radiotherapy; reflectance confocal microscopy; surgery.

Radiation therapy (RT) is a treatment option for select skin cancers in patients unwilling or unable to undergo surgical resection. Despite the fact that ionizing RT has been used for more than a century, its histologic effects on human skin are still ill defined. Moreover, serial skin biopsies would disrupt the natural evolution of skin post-RT effects.

Basal cell carcinoma (BCC) is the most common skin malignancy.[1,2] Multiple adjunctive noninvasive imaging modalities have emerged to aid in determining the extent of BCC that may also help in the assessment of response to therapy. Dermoscopy uses magnification to enhance BCC detection.[3-5] High-frequency ultrasonography (HFUS) uses sound waves to provide a vertical field of view that can extend through the entire thickness of skin to subcutaneous tissues.[6] Finally, reflectance confocal microscopy (RCM) detects backscattered light from brightly illuminated tissues to provide an en face view up to 200 to 250 μm.[7-15]

The objective of this study was to describe the tumoral and stromal changes observed in patients with BCC treated with high-dose ionizing RT at different timepoints. To the best of our knowledge, no prior study has attempted to comprehensively characterize skin cancers before and after RT using dermoscopy, HFUS, and RCM.

CAPSULE SUMMARY

- Noninvasive imaging tools such as dermoscopy, reflectance confocal microscopy, and high-frequency ultrasonography were used to monitor basal cell carcinoma and tissue response to radiation therapy.
- In the future, patients undergoing nonsurgical modalities, such as radiation therapy, may benefit from these emerging noninvasive diagnostic modalities to guide and monitor treatment.

PATIENTS AND METHODS

This was an institutional review board–approved, prospective pilot clinical trial (14-001, NCT02131805). All patients provided informed consent. The enrollment of participants occurred between 2014 and 2018.

Inclusion criteria

Patients 60 years and older with biopsy-proven, early-stage (T1N0M0 according to American Joint Committee for Cancer, 7th edition staging criteria) BCC with no high-risk features on biopsy (perineural invasion, >2-mm thickness, ≤1 cm for histologic high-risk BCC subtypes) not willing or unable to undergo surgery.

Exclusion criteria

Patients with recurrent BCCs; BCCs in areas of prior RT; nonaccessible surfaces (eg, intraconchal); and BCCs adjacent to or overlapping burns, scars, or areas of compromised lymphovascular drainage were excluded. Patients with a predisposition to adverse events from RT were also not eligible.

Radiation therapy

RT was delivered with a commercially available electronic skin surface brachytherapy unit operating at 69.5 kV (Esteya, Nucletron, Elekta Brachytherapy, Veenendaal, the Netherlands). The dose profiles for this treatment unit have been previously reported.[16] A total dose of 42 Gy was delivered to 3 mm below the skin surface in 6 fractions of 7 Gy. This dose was given on nonconsecutive days over no more than 21 days (2 or 3 fractions per workweek; nonconsecutive days). The gross tumor was identified by visual inspection. Applicators 10 to 30 mm in diameter, with a goal of 4 mm of clear margin (radial expansion) were used to deliver radiation. For high-risk histologic BCC subtypes, 10 mm of radial expansion was used.

Evaluations

Patients were evaluated before treatment and then at 6 weeks, 3 months, and 12 months after treatment. At each evaluation digital photography, dermoscopy, RCM, and HFUS were performed to assess tumoral and tissue response in vivo. To describe the natural pathophysiologic evolution of RT-related skin changes, biopsies of the irradiated skin were not performed during the study unless there was clinical suspicion of recurrence. After the

Abbreviations used:

BCC: basal cell carcinoma
HFUS: high-frequency ultrasonography
RCM: reflectance confocal microscopy
RT: radiation therapy

12-month protocol, patients continued clinical follow-up as per the standard of care.

Digital photography and dermoscopy

Photos were taken with a digital camera (Canfield Imaging Systems, NJ). Digital dermoscopy was performed with the VEOS DS3 (Canfield Imaging Systems, NJ), with polarized and nonpolarized images acquired. Dermoscopic images were retrospectively analyzed for consensus by 3 dermatologists. Images were analyzed for previously described BCC criteria, predominant dermoscopic color, and increased background vessels (Table I).[4,17-20]

RCM

Handheld RCM was used (VivaScope 3000, Caliber ID, Rochester, NY); lesions were outlined with specially designed paper rings.[21] The RCM imaging protocol included single images, stacks (from the corneal layer up to 250 μm) in the center of the lesion, and 6 videos: 2 across the lesion and 4 clockwise at the peripheral margin of each quadrant.

RCM images were retrospectively evaluated for consensus by 3 investigators. We evaluated BCC features as previously described (Table I).[22] Additionally, we described 4 new RCM features observed in irradiated-tissue (Fig 1): radiation-associated epidermal atypia (atypical morphology and arrangement of keratinocytes in the epidermis), perifollicular fibrosis (bright collagen around hair follicles), large bright spots (poorly defined bright structures with no triangular shape and no nucleus in the dermis), and fading tumor (tumor-like areas at the DEJ or dermis where clear-cut tumor was seen before). We also evaluated the presence of a recently described criterion termed *trapped epidermis* (well-defined hyperreflective nodules composed of normal keratinocytes only, without palisading and clefting, which differentiates them from BCC nodules).[19]

For HFUS protocol and methods, see the Supplemental Material (available via Mendeley at http://dx.doi.org/10.17632/x92rzty5vw.1).

Statistical analysis

Descriptive statistics including mean, median, range, standard deviation, and relative frequency were used to describe the study participants; characteristics of the tumors; and RCM, dermoscopic, and HFUS characteristics. For subtype analysis, cases were grouped as low risk (superficial and nodular) and high risk (infiltrative, micronodular, nodulocystic). To compare categorical variables, the chi-square test was used. A 2-tailed P value of less than .05 was considered statistically significant. Data were analyzed with SPSS 23.0 (Armonk, NY).

RESULTS

A total of 137 independent imaging assessments (RCM + dermoscopy + HFUS) were performed in 13 patients. One patient died of unrelated causes before study completion and was excluded from further analysis. The mean age at diagnosis was 77.0 years (standard deviation, 10.7; range, 60-94 y). Ten patients (83.3%) were women. All BCCs were located on the head and neck; 8 lesions on the nose, 1 on the forehead, 1 on the chin, 1 on the glabella, and 1 on the preauricular area. BCC subtypes were as follows: 6 nodular, 2 infiltrative, 1 micronodular, 1 nodulocystic, and 1 superficial; 1 was not specified. No patient had clinical evidence of recurrence during follow-up; hence, no biopsies were performed during the study. The mean follow-up time was 31.7 months (range, 23-47 months).

Dermoscopy

Forty-one dermoscopic image sets from 12 patients were analyzed; 7 dermoscopic images were not available for analysis. Dermoscopy showing BCC-specific features was more common at baseline than during subsequent follow-up (Table I). However, only the presence of arborizing vessels became less notable during follow-up (P = .032). Orange color emerged during the 6-week and 3-month follow-ups (P = .128) as well as the gradual increase of white color from baseline to the 12-month follow-up (from 18.1% to 55.5%; P = .313).

RCM

Forty-eight confocal studies were performed in 12 patients. RCM showed BCC-specific criteria in 11 of 12 (91.7%) lesions at baseline. At the 6-week, 3-month, and 12-month follow-ups, only 1 patient (8.3%) showed BCC features under RCM. No patients showed clinical signs (ie, naked-eye examination) of recurrence after 1 year of follow-up, and therefore, no biopsies were performed (Table I and Fig 2).

BCC-specific features (nodules and cordlike structures) were the most common finding at baseline (75.0% and 66.7%; P = .001 and <.001, respectively). There were no differences between low-risk and high-risk BCC subtypes at baseline (see

Table I. RCM and dermoscopic features seen at different timepoints (n = 12)

Imaging features	Baseline (n, %)	6 weeks (n, %)*	3 months (n, %)	12 months (n, %)	*P* value
RCM features					
Suprabasal epidermis features					
Atypical honeycomb†	4 (33.3)	7 (63.6)	8 (66.7)	2 (16.7)	**.039**
Streaming	4 (33.3)	0	0	0	**.007**
Epidermal dendritic cells	4 (33.3)	9 (81.8)	5 (41.7)	4 (33.3)	.063
DEJ/superficial dermis features					
Cordlike structures	8 (66.7)	0	0	0	**<.001**
Bright nucleated cells in the DEJ	0	7 (63.6)	6 (50.0)	3 (25.0)	**.006**
Tumor nodules	9 (75.0)	1 (9.1)	1 (8.3)	1 (8.3)	**.001**
Palisading	11 (91.7)	1 (9.1)	0 (0)	1 (8.3)	**<.001**
Clefting	9 (75.0)	1 (9.1)	1 (8.3)	1 (8.3)	**<.001**
Intratumoral dendritic cells	2 (18.2)	1 (9.1)	0	0	.252
Dark silhouettes	0	0	0	0	N/A
Horizontal vessels	9 (75)	8 (72.7)	9 (75.0)	7 (58.3)	.776
Vertical vessels	1 (8.3)	4 (36.4)	3 (25.0)	6 (54.5)	.105
Plump cells	3 (25.0)	6 (66.7)	8 (66.7)	1 (8.3)	**.009**
Inflammatory cells	9 (75.0)	8 (72.7)	10 (83.3)	3 (27.3)	**.023**
Fading tumor	0	4 (40.0)	3 (25.0)	4 (33.3)	.122
Fibrosis	4 (33.3)	8 (72.7)	10 (83.3)	12 (100.0)	**.002**
Reticular collagen	2 (16.7)	7 (63.6)	10 (83.3)	5 (41.7)	**.008**
Amorphous collagen	3 (25.0)	3 (27.3)	9 (75.0)	12 (100)	**<.001**
Perifollicular fibrosis	0	2 (18.2)	3 (25.0)	8 (66.7)	**.003**
Trapped epidermis	1 (8.3)	8 (72.7)	9 (75.0)	9 (75.0)	**.001**
Bright nucleated cells in the dermis	0	6 (54.5)	3 (25.0)	1 (8.3)	**.008**
Large bright spots	0	6 (54.5)	6 (54.5)	3 (25.0)	**.012**
	Baseline (n, %)‡	**6 weeks (n, %)§**	**3 months (n, %)‖**	**12 months (n, %)¶**	
Dermoscopic features					
Arborizing vessels	3 (27.2)	0	0	0	**.032**
Blue-gray globules	1 (9.1)	0	0	0	.424
Blue-gray ovoid nests	1 (9.1)	0	0	0	.424
Short fine telangiectasia	6 (54.5)	3 (30)	3 (27.2)	1 (11.1)	.210
Spoke wheel areas	0	0	0	0	N/E
Concentric structures	0	0	0	0	N/E
Leaf like structures	0	0	0	0	N/E
In-focus dots	1 (9.1)	0	0	0	.424
Ulceration	1 (9.1)	0	0	0	.424
Shiny white blotches and strands	9 (81.8)	8 (80)	9 (81.8)	6 (66.6)	.829
Peppering	0	1 (10)	1 (9.1)	0	.542
Background vessels	0	0	1 (9.1)	2 (22.2)	.199
Scale	0	1 (10)	0	2 (22.2)	.188
Rosettes	3 (27.2)	1 (10)	1 (9.1)	0	.227
Predominant color					
Pink	9 (81.8)	5 (50)	3 (27.2)	4 (44.4)	.078
White	2 (18.1)	3 (30)	5 (45.4)	5 (55.5)	.313
Orange	0	2 (20)	3 (27.2)	0	.128

Bold values indicate *P* values <.05.

DEJ, Dermoepidermal junction; *N/E*, not evaluable; *RCM*, reflectance confocal microscopy.

*One patient missed the 6-week RCM follow-up (n = 11 for that evaluation).

†Includes radiation-associated epidermal atypia.

‡Dermoscopic analysis based on 11 evaluations (1 missing dermoscopic image).

§Dermoscopic analysis based on 10 evaluations (2 missing dermoscopic images).

‖Dermoscopic analysis based on 11 evaluations (1 missing dermoscopic image).

¶Dermoscopic analysis based on 9 evaluations (3 missing dermoscopic images).

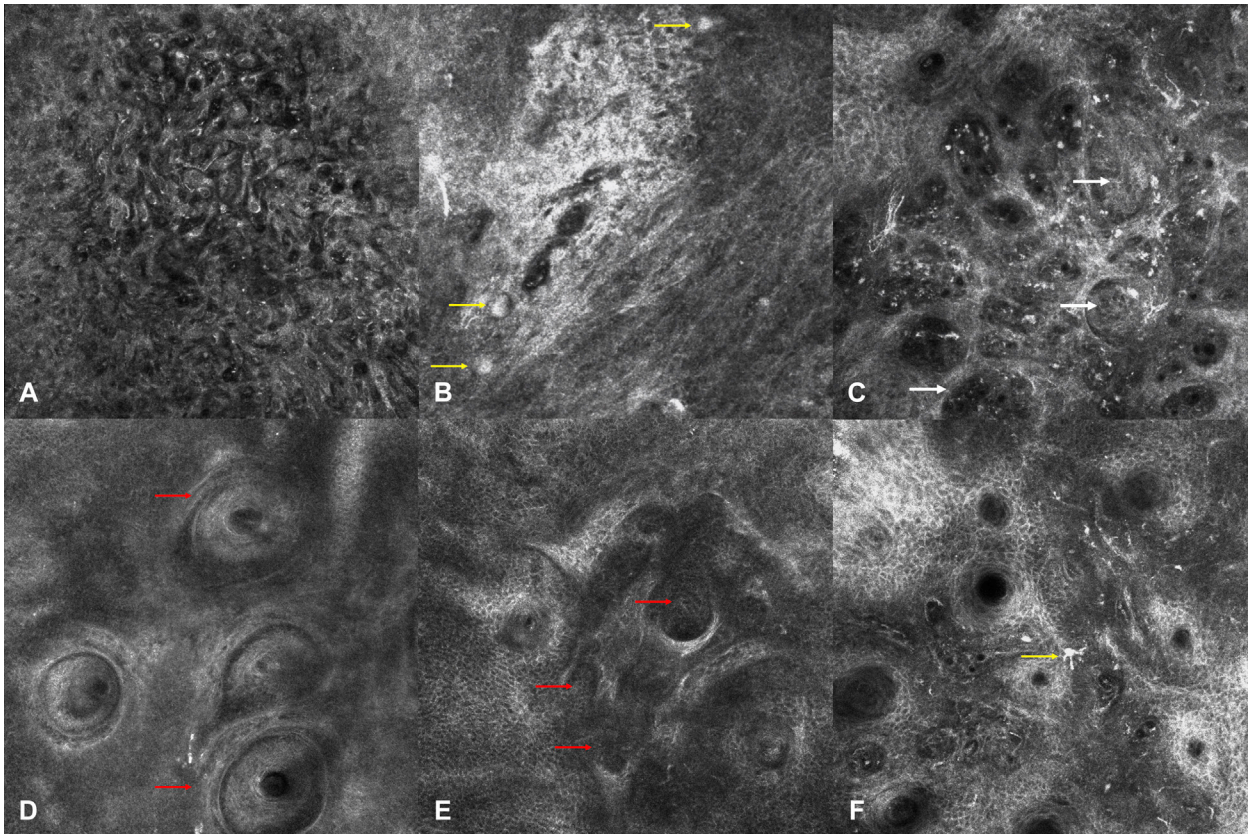

Fig 1. Radiation therapy–associated reflectance confocal microscopy features. **A**, Radiation-associated epidermal atypia seen at 6 weeks after initial radiation therapy (750 × 750 μm). **B**, Large bright spots (yellow arrows) seen at the 3-month follow-up (750 × 750 μm). **C**, Fading tumor (white arrows) amidst a background of inflammatory and dendritic cells seen at the 6-week follow-up. (750 × 750 μm). **D**, Perifollicular fibrosis (red arrows) seen at the 12-month follow-up (750 × 750 μm). **E**, Trapped epidermis (red arrows) seen at the 12-month follow-up (750 × 750 μm). **F**, Epidermal dendritic cell (yellow arrow), seen at 3 month-follow-up (750 × 750 μm).

Supplemental Material). Inflammatory features and atypical honeycomb (including radiation-associated epidermal atypia) predominated in the 6-week and 3-month follow-ups (epidermal dendritic cells, plump-cells, inflammatory cells, and atypical honeycomb; P = .063, .009, .023, and .039, respectively). At the 12-month follow-up, features suggestive of fibrosis and vertical vessels were seen (P = .002 and .105, respectively). BCC-specific features and inflammatory features diminished to less than 30% at the 12-month follow-up (Table I and Fig 2). No differences were found between low-risk and high-risk BCCs and RCM features during follow-up (see Supplemental Material). There was no association between the type of clinically noted adverse effects and the RCM findings (data not shown). Representative imaging is presented in Figs 3 and 4.

For HFUS results, see the Supplemental Material.

DISCUSSION

RT has a long history in the treatment of skin cancers and is a treatment option for select BCCs.[2,23-25] The main limitation of RT, when compared to surgery, is the lack of histopathologic confirmation of clearance. In this prospective, preliminary study, we performed 137 independent imaging assessments (RCM + dermoscopy + HFUS) and observed that RCM could possibly enable the evaluation of the pathophysiologic effects of high-dose ionizing radiation in the skin, without the need for disruption of the skin architecture with repeated biopsies. RCM positivity for BCC decreased from 91.7% at baseline to 8.3% at the 12-month follow-up.

This study provided real-time analysis of RT tissue response. We were able to describe, by means of RCM, quasi-histologic features seen at different

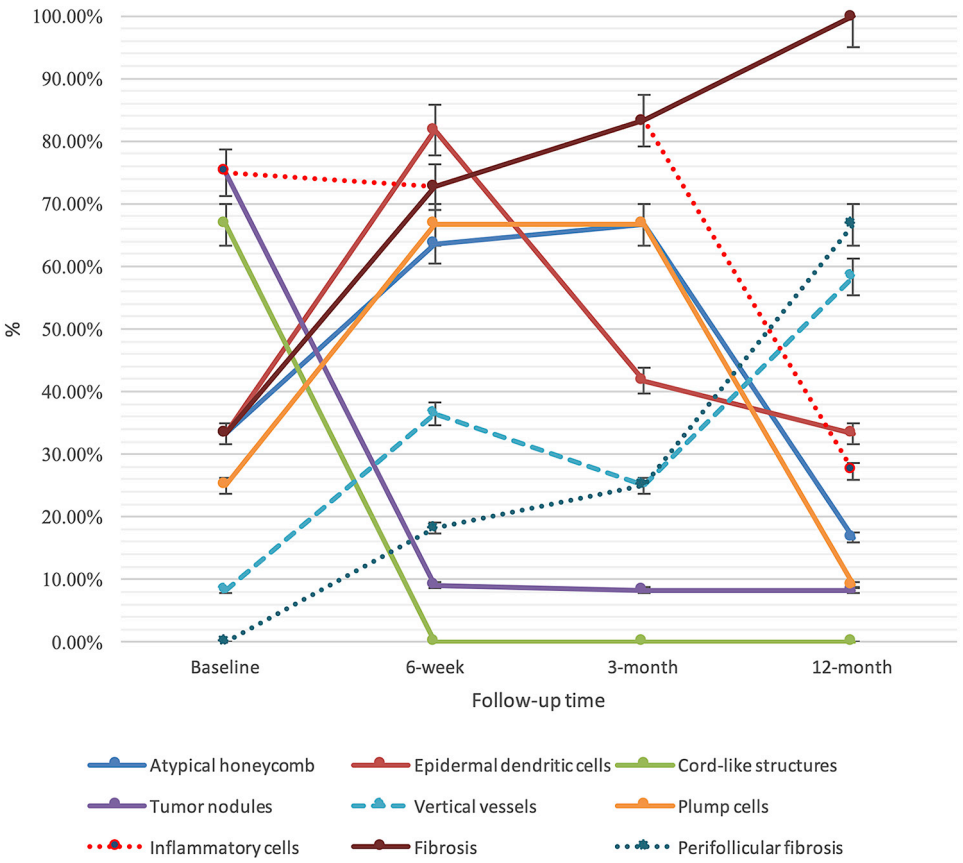

Fig 2. Reflectance confocal microscopy features seen across time in the study patients. Error bars represent standard deviation.

timepoints in irradiated patients (Fig 2). The main RCM findings included atypical honeycomb peaking in the first 3 months of follow-up, which we termed *radiation-associated epidermal atypia*. It most probably corresponds to a form of radiation dermatitis visualized under RCM.[26] As expected, this epidermal feature was minimal at the 12-month follow-up, when acute dermatitis resolved. Additionally, we observed a peak of epidermal dendritic cells (possibly Langerhans cells) in the first 3 months (up to 82%); this decreased to 33% at 12 months.[27] This observation corroborates previous findings of increased epidermal dendritic cells after RT for lentigo maligna.[14,28] Melanophages (plump cells) peaked during the first 3 months after RT. The presence of these changes provides undescribed insights into the pattern of skin immunologic response to RT.

RCM features of fibrosis were seen in all patients 1 year after RT. Clinically, the observation of fibrosis often takes longer than 1 year, suggesting that RCM may be able to detect earlier, subclinical manifestations of fibrosis. Interestingly, we were able to visualize, in vivo, the variations in collagen shape during the 12-month period. Fibrosis was present in only 33% of patients, and during the first 3 months, collagen was mainly reticular. At the 12-month follow-up, collagen was primarily amorphous with perifollicular fibrosis. These changes in the collagen shape visualized under RCM may correlate with the different subtypes of collagen expressed during tissue healing after RT.[29]

In concordance with previous studies evaluating biopsied/treated lesions, dermoscopy was not very helpful in evaluating the presence or absence of residual BCC.[19] The only dermoscopic feature with potential relevance was the presence of arborizing vessels, typically seen in nodular BCC[5,30]; however, only 6 of our patients had disease of the nodular subtype. In addition, other BCC-specific dermoscopic features, such as short, fine telangiectasias and shiny white blotches and strands, lose validity in biopsied lesions because they can also be seen in scars.[19] An interesting feature was the visualization of orange color and peppering. Orange color and peppering have both been described in lichen planus–like keratosis, which typically presents with a dense lichenoid infiltrate on histopathology.[31] We hypothesize that the orange color and peppering

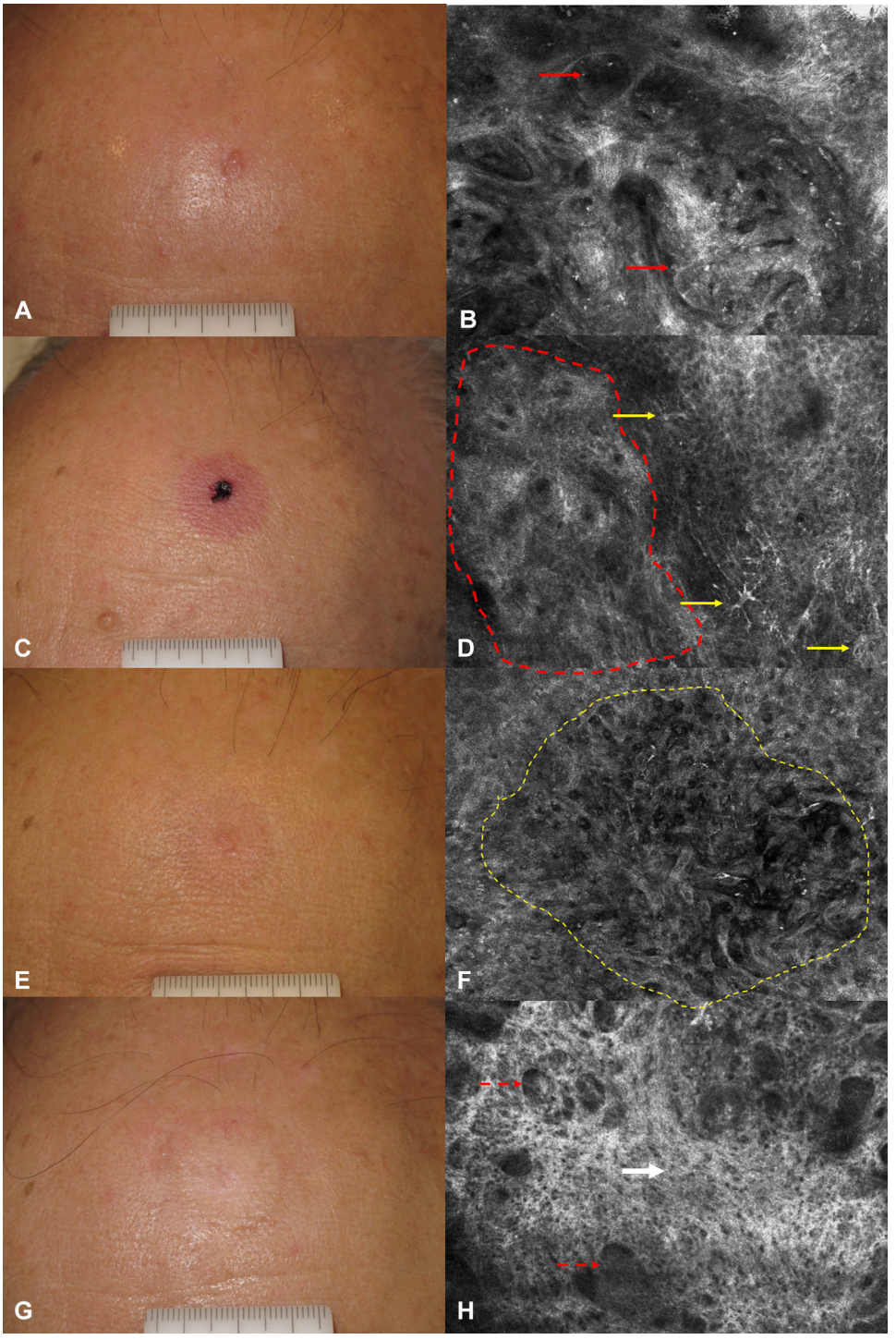

Fig 3. Micronodular basal cell carcinoma on the forehead. **A**, Baseline clinical picture showing a 0.5-cm pink papule. **B**, Baseline RCM image showing tumor nodules and cords with palisading and clefting (red arrows) (750 × 750 μm). **C**, The 6-week follow-up, clinical photo. **D**, RCM image showing bright nucleated dendritic cells in the epidermis (yellow arrows) and fading tumor (red dashed outline) (750 × 750 μm). **E**, The 3-month follow-up, clinical photo. **F**, RCM image showing an atypical honeycomb pattern, typically seen in the radiation-associated epidermal atypia (dashed yellow outline) (750 × 750 μm). **G**, The 12-month follow-up, clinical photo. **H**, RCM image showing fibrosis with an amorphous collagen (white arrow) and trapped epidermis (red dashed arrows) mimicking tumor nodules (750 × 750 μm). *RCM*, Reflectance confocal microscopy.

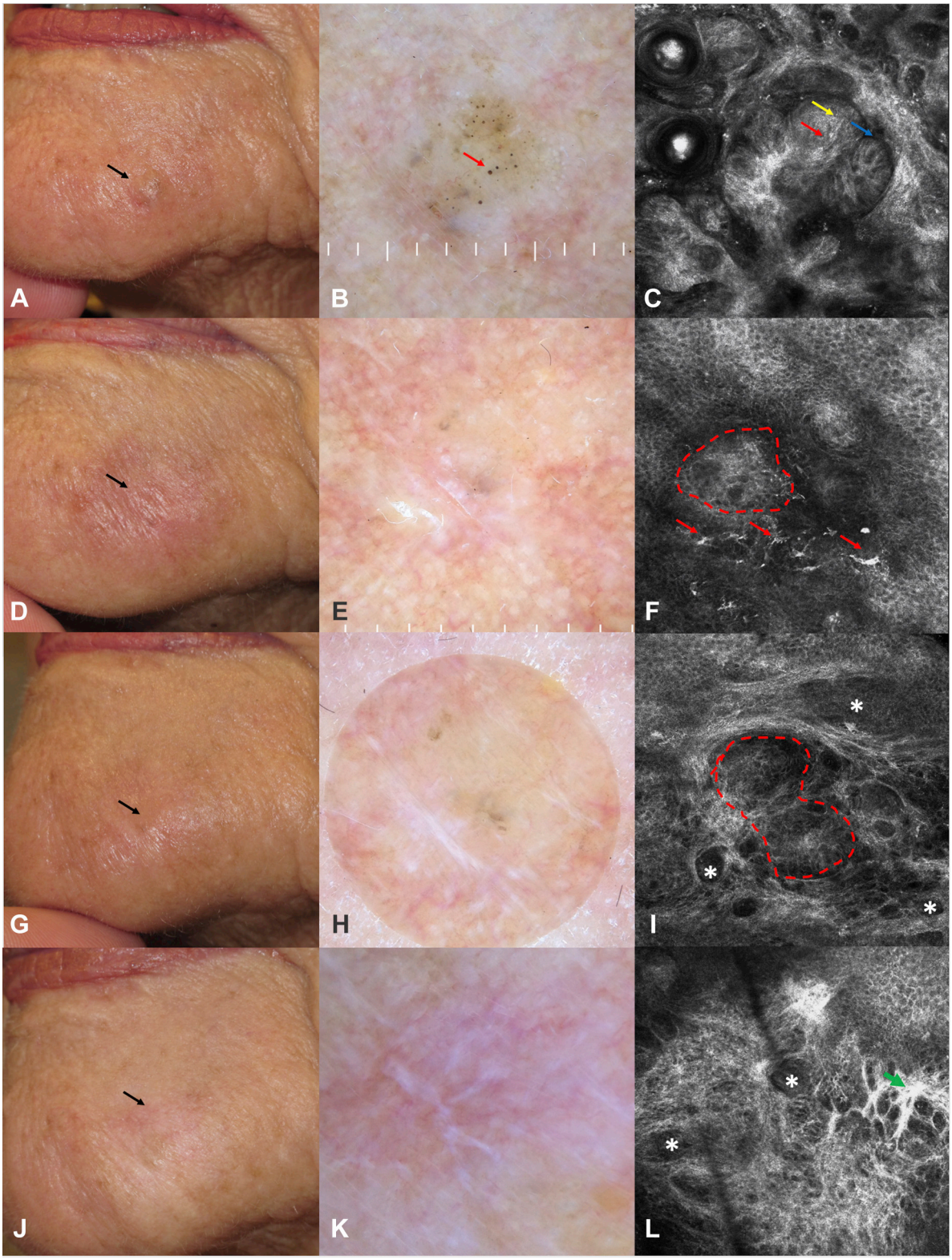

Fig 4. Pigmented basal cell carcinoma on the chin. **A**-**C**, Baseline. **A**, Clinical features (black arrow). **B**, Dermoscopic image showing in-focus dots (red arrow) and blue-gray globules (polarized-light dermoscopy; original magnification: ×10). **C**, RCM image showing tumor nodules (red arrow) with palisading (yellow arrow) and clefting (blue arrow) (750 × 750 μm). **D**—**F**, The 6-week follow-up. **D**, Clinical features. **E**, Dermoscopic features showing blotches

seen in our cases during the 6-week and 3-month follow-ups are the dermoscopic counterpart of the RCM plump cells, inflammatory cells, and epidermal dendritic cells. On the other hand, the visualization of white color under dermoscopy most probably corresponds to fibrosis under RCM.[32]

Limitations

The main limitation of our study was the lack of histopathologic correlation; however, patients electing to have noninvasive treatment would have likely declined the 4 timepoint biopsies. Moreover, the objective of our study was to describe the response of patients receiving RT longitudinally in vivo. Biopsies would have caused inflammation and scarring that may have obscured the natural pathophysiologic evolution and changes after RT. In the future, small tissue biopsies (targeted) could be undertaken to correlate the newly described RCM findings reported here.[33] Because no patient presented with clinically evident recurrent disease after a mean follow-up of 31.7 months, biopsies were not performed. An additional limitation of our study was the relatively small patient sample size, which impedes subanalysis by location and definitive conclusions on subtype. However, our study incorporated 137 independent imaging modality timepoints, thereby providing a comprehensive in vivo evaluation of BCC and tissue response to RT. There was no control group to evaluate whether changes seen on dermoscopy and RCM are related to tumor resolution or RT only; comparison with other noninvasive therapies (eg, imiquimod) could further elucidate this. Finally, there is wide clinical variability in BCC appearance, which can modify noninvasive imaging appearance.

CONCLUSION

RCM could prove to be a valuable tool in the noninvasive evaluation of patients with BCC treated with RT; we were able to successfully observe the tissue response to RT in vivo. In the future, RCM may help monitor the in vivo response of BCC to RT or other nonsurgical modalities.

REFERENCES

1. Rogers HW, Weinstock MA, Feldman SR, Coldiron BM. Incidence estimate of nonmelanoma skin cancer (keratinocyte carcinomas) in the U.S. population, 2012. *JAMA Dermatol*. 2015;151:1081-1086.
2. National Comprehensive Cancer Network. Basal cell skin cancer (version 1.2018); 2018. Accessed January 1, 2019. https://www.nccn.org/professionals/physician_gls/pdf/nmsc.pdf
3. Wortsman X, Vergara P, Castro A, et al. Ultrasound as predictor of histologic subtypes linked to recurrence in basal cell carcinoma of the skin. *J Eur Acad Dermatol Venereol*. 2015;29:702-707.
4. Navarrete-Dechent C, Bajaj S, Marchetti MA, Rabinovitz H, Dusza SW, Marghoob AA. Association of shiny white blotches and strands with nonpigmented basal cell carcinoma: evaluation of an additional dermoscopic diagnostic criterion. *JAMA Dermatol*. 2016;152:546-552.
5. Lallas A, Tzellos T, Kyrgidis A, et al. Accuracy of dermoscopic criteria for discriminating superficial from other subtypes of basal cell carcinoma. *J Am Acad Dermatol*. 2014;70:303-311.
6. Dinnes J, Bamber J, Chuchu N, et al. High-frequency ultrasound for diagnosing skin cancer in adults. *Cochrane Database Syst Rev*. 2018;(12):CD013188.
7. Kadouch DJ, Schram ME, Leeflang MM, Limpens J, Spuls PI, de Rie MA. In vivo confocal microscopy of basal cell carcinoma: a systematic review of diagnostic accuracy. *J Eur Acad Dermatol Venereol*. 2015;29:1890-1897.
8. Rajadhyaksha M, Marghoob A, Rossi A, Halpern AC, Nehal KS. Reflectance confocal microscopy of skin in vivo: from bench to bedside. *Lasers Surg Med*. 2017;49:7-19.
9. Torres A, Niemeyer A, Berkes B, et al. 5% imiquimod cream and reflectance-mode confocal microscopy as adjunct modalities to Mohs micrographic surgery for treatment of basal cell carcinoma. *Dermatol Surg*. 2004;30:1462-1469.
10. Pasquali P, Segurado-Miravalles G, Freites-Martinez A, Gonzalez-Rodriguez S. Cryosurgical management of basal cell carcinoma: in vivo follow-up using reflectance confocal microscopy. *Int J Dermatol*. 2019;58:e30-e32.
11. Hibler BP, Sierra H, Cordova M, et al. Carbon dioxide laser ablation of basal cell carcinoma with visual guidance by reflectance confocal microscopy: a proof-of-principle pilot study. *Br J Dermatol*. 2016;174:1359-1364.
12. Sierra H, Yelamos O, Cordova M, Chen CJ, Rajadhyaksha M. Reflectance confocal microscopy-guided laser ablation of basal cell carcinomas: initial clinical experience. *J Biomed Opt*. 2017;22:1-13.
13. Sierra H, Cordova M, Chen CJ, Rajadhyaksha M. Confocal imaging-guided laser ablation of basal cell carcinomas: an ex vivo study. *J Invest Dermatol*. 2015;135:612-615.

and strands and regression structures (polarized-light dermoscopy; original magnification: ×10). **F**, RCM features showing fading tumor (red dashed outline) and bright, large, nucleated dendritic cells in the epidermis (red arrows), most probably corresponding to Langerhans cells (750 × 750 μm). **G–I**, The 3-month follow-up. **G**, Clinical features (black arrow). **H**, Dermoscopic features showing blotches and strands and regression structures (polarized-light dermoscopy; original magnification: ×10). **I**, RCM features showing fading tumor (red dashed outline) and trapped epidermis (white asterisks) (750 × 750 μm). **J–L**, The 12-month follow-up. **J**, Clinical features. **K**, Dermoscopic features showing only blotches and strands and white-pink background (polarized-light dermoscopy; original magnification: ×10). **L**, RCM features showing fibrosis (green arrows) and trapped epidermis (white asterisks) (750 × 750 μm). *RCM*, Reflectance confocal microscopy.

14. Richtig E, Arzberger E, Hofmann-Wellenhof R, Fink-Puches R. Assessment of changes in lentigo maligna during radiotherapy by in-vivo reflectance confocal microscopy: a pilot study. *Br J Dermatol*. 2015;172:81-87.
15. Navarrete-Dechent C, Cordova M, Liopyris K, et al. Reflectance confocal microscopy-guided carbon dioxide laser ablation of low-risk basal cell carcinomas: a prospective study. *J Am Acad Dermatol*. 2019;81:984-988.
16. Garcia-Martinez T, Chan JP, Perez-Calatayud J, Ballester F. Dosimetric characteristics of a new unit for electronic skin brachytherapy. *J Contemp Brachytherapy*. 2014;6:45-53.
17. Menzies SW, Westerhoff K, Rabinovitz H, Kopf AW, McCarthy WH, Katz B. Surface microscopy of pigmented basal cell carcinoma. *Arch Dermatol*. 2000;136:1012-1016.
18. Kittler H, Marghoob AA, Argenziano G, et al. Standardization of terminology in dermoscopy/dermatoscopy: results of the third consensus conference of the International Society of Dermoscopy. *J Am Acad Dermatol*. 2016;74:1093-1106.
19. Navarrete-Dechent C, Cordova M, Aleissa S, et al. Reflectance confocal microscopy confirms residual basal cell carcinoma on clinically negative biopsy sites before Mohs surgery: a prospective study. *J Am Acad Dermatol*. 2019;81:417-426.
20. Banuls J, Arribas P, Berbegal L, DeLeon FJ, Frances L, Zaballos P. Yellow and orange in cutaneous lesions: clinical and dermoscopic data. *J Eur Acad Dermatol Venereol*. 2015;29:2317-2325.
21. Marino ML, Rogers T, Sierra Gil H, Rajadhyaksha M, Cordova MA, Marghoob AA. Improving lesion localization when imaging with handheld reflectance confocal microscope. *Skin Res Technol*. 2016;22:519-520.
22. Navarrete-Dechent C, DeRosa AP, Longo C, et al. Reflectance confocal microscopy terminology glossary for nonmelanocytic skin lesions: a systematic review. *J Am Acad Dermatol*. 2019;80:1414-1427.
23. Telfer NR, Colver GB, Morton CA, British Association of Dermatologists. Guidelines for the management of basal cell carcinoma. *Br J Dermatol*. 2008;159:35-48.
24. Peris K, Fargnoli MC, Garbe C, et al. Diagnosis and treatment of basal cell carcinoma: European consensus-based interdisciplinary guidelines. *Eur J Cancer*. 2019;118:10-34.
25. Work Group, Invited Reviewers, Kim JYS, Kozlow JH, Mittal B, et al. Guidelines of care for the management of basal cell carcinoma. *J Am Acad Dermatol*. 2018;78:540-559.
26. Vano-Galvan S, Fernandez-Lizarbe E, Truchuelo M, et al. Dynamic skin changes of acute radiation dermatitis revealed by in vivo reflectance confocal microscopy. *J Eur Acad Dermatol Venereol*. 2013;27:1143-1150.
27. Hashemi P, Pulitzer MP, Scope A, Kovalyshyn I, Halpern AC, Marghoob AA. Langerhans cells and melanocytes share similar morphologic features under in vivo reflectance confocal microscopy: a challenge for melanoma diagnosis. *J Am Acad Dermatol*. 2012;66:452-462.
28. Hibler BP, Connolly KL, Cordova M, Nehal KS, Rossi AM, Barker CA. Radiation therapy for synchronous basal cell carcinoma and lentigo maligna of the nose: response assessment by clinical examination and reflectance confocal microscopy. *Pract Radiat Oncol*. 2015;5:e543-e547.
29. Keskikuru R, Jukkola A, Nuutinen J, et al. Radiation-induced changes in skin type I and III collagen synthesis during and after conventionally fractionated radiotherapy. *Radiother Oncol*. 2004;70:243-248.
30. Longo C, Lallas A, Kyrgidis A, et al. Classifying distinct basal cell carcinoma subtype by means of dermatoscopy and reflectance confocal microscopy. *J Am Acad Dermatol*. 2014;71:716-724.
31. Liopyris K, Navarrete-Dechent C, Dusza SW, et al. Clinical and dermoscopic features associated with lichen planus-like keratoses that undergo skin biopsy: a single-center, observational study. *Australas J Dermatol*. 2019;60:e119-e126.
32. Liopyris K, Navarrete-Dechent C, Yelamos O, Marchetti MA, Rabinovitz H, Marghoob AA. Clinical, dermoscopic and reflectance confocal microscopy characterization of facial basal cell carcinomas presenting as small white lesions on sun-damaged skin. *Br J Dermatol*. 2019;180:229-230.
33. Navarrete-Dechent C, Liopyris K, Cordova M, Busam KJ, Marghoob AA, Chen CJ. Reflectance confocal microscopic and en face histopathologic correlation of the dermoscopic "circle within a circle" in lentigo maligna. *JAMA Dermatol*. 2018;154:1092-1094.